SCIENCE CHINA
Technological Sciences

Special Topic: Neurodynamics and Network Science
•Article•

July 2022 Vol.65 No.7: 1445–1455
https://doi.org/10.1007/s11431-021-2042-4

Traveling chimera states in locally coupled memristive Hindmarsh-Rose neuronal networks and circuit simulation

YUAN YuanYuan, YANG Hao, HAN Fang* & WANG ZhiJie

College of Information Science and Technology, Donghua University, Shanghai 201620, China

Received December 16, 2021; accepted March 25, 2022; published online June 16, 2022

Chimera states have been found in many physiology systems as well as nervous systems and may relate to neural information processing. The present work investigates the traveling chimera states in memristive neuronal networks of locally coupled Hindmarsh-Rose neurons, with both excitation and inhibition considered. Various traveling chimera patterns and firing modes are found to exist in the networks. Particularly, for excitatory connection, two kinds of traveling chimera states appear in opposite directions. Besides, a new type of chimera state composed of traveling chimera state and incoherent state is observed, named the semi-traveling chimera state. Multi-head traveling chimera states with several incoherent groups are also observed. For excitatory-inhibitory connection, the network is observed to exhibit an imperfect coherent state under the synergistic effect of strong excitatory and weak inhibitory coupling. Moreover, a firing pattern named mixed-amplitude bursting state is witnessed, consisting of two bursts of different amplitudes in a time sequence. Furthermore, an electric circuit is designed and built on Multisim to realize the above phenomena, suggesting that traveling chimera states could be generated in real circuits. Our findings can deepen the understanding of the electromagnetic induction effect in regulating the dynamics of neuronal networks and may provide useful clues for constructing artificial neural systems.

memristive neuronal network, traveling chimera state, firing pattern, electric circuit

Citation: Yuan Y Y, Yang H, Han F, et al. Traveling chimera states in locally coupled memristive Hindmarsh-Rose neuronal networks and circuit simulation. Sci China Tech Sci, 2022, 65: 1445–1455, https://doi.org/10.1007/s11431-021-2042-4

1 Introduction

Chimera states are counter-intuitive and symmetry-broken spatiotemporal patterns that exist in identical coupled oscillators, in which the coherent and incoherent dynamics coexist. Since this phenomenon was discovered by Kuramoto and Battogtokh [1] in nonlocally coupled phase oscillators in 2002, it has been studied extensively in physics, biology, and chemistry. In addition to the earliest findings of chimera states in nonlocally coupled networks [1–3], recent studies have also demonstrated the existence of chimera states in globally [4,5] and locally [6–8] coupled networks. The different types of chimera states are classified into several categories according to the spatiotemporal dynamics of oscillators, including the traveling, multi-head, and imperfect chimera states [8–10]. And depending on the symmetry breaking situations in networks, chimera states are also named amplitude chimera state [11] and chimera death [12]. Recently, chimera states have been observed in many networks of different structures, and other factors that may affect the existence of chimera states, such as the coupling mode, node dynamics, and time delay, were also studied deeply [13–15].

Chimera state is found in the nervous system and may be involved in neural information processing. The *unihemispheric slow-wave sleep* phenomenon discovered in some birds and mammals indicates that half of the brain is synchronous, and the other half is asynchronous when they fall

*Corresponding author (email: yadiahan@dhu.edu.cn)

asleep. The existence of chimera state has also been found in the human cerebral cortex by using magnetic resonance imaging (MRI) technology to scan the human brain when the subject is involved in a specific activity [16]. Furthermore, researchers constructed connection matrices based on the *C. Elegans* soil worm connectome [17] and the cerebral cortex of cats [18] and observed chimera states in networks. In recent years, reports in various neuronal models, including Leaky Integrate-and-Fire oscillators [19], Hindmarsh-Rose oscillators [20–23], FitzHugh-Nagumo oscillators [24,25], and several other neuron models, have also revealed that chimera states can appear in neuronal networks. Majhi et al. [26] studied a locally coupled two-layer network of excitatory Hindmarsh-Rose neurons and demonstrated the generation of chimera states in the uncoupled layer. Bera et al. [21] reported chimera states in excitatory synaptic coupled Hindmarsh-Rose neuronal network with local, nonlocal, and global couplings, thereby proving that nonlocal coupling is not a necessary condition for the emergence of a chimera state.

Furthermore, excitation-inhibition balance plays an important role in information transfer in the brain and may relate to the cognition of the nervous system [27]. Some research studies regarding the chimera states in neuronal networks with both excitatory and inhibitory connections have emerged. Belykh et al. [28] reported that the synergy of excitation and inhibition can make the system completely synchronized. Bera et al. [9] built a neuronal network with local and gradient coupling and found an imperfect traveling chimera state in the network of excitatory-inhibitory coupled Hindmarsh-Rose neurons.

Electromagnetic fields exist in the neural system, and there is also an energy dissipation in neurons [29]. Thus, Ma and Tang [30] introduced the memristor model into neurons. In recent years, the memristor model has attracted much attention and has been widely studied. Some researchers utilized a composite system made of memristors and neurons to achieve synaptic functions, thus providing a foundation for further research on the dynamics of memristive synapses [31,32]. Complex chaotic dynamics can appear in memristive neuronal networks. Korneev et al. [33] constructed a ring locally coupled memristive neuronal network and explored the influence of the initial state of the memristors on the waveform and wave propagation velocity. Chimera states have also been reported in the memristive neuronal network of coupled Hindmarsh-Rose neurons [34,35]. Xu et al. [36] constructed a two-layer neuronal network based on memristive synapses and studied the influence of electromagnetic induction on the dynamics of neuronal networks along with discovering traveling chimera states.

However, almost no work has reported the existence of chimera states in memristive neuronal networks wherein excitation and inhibition coexist. Therefore, in this paper, we construct a ring network composed of identical Hindmarsh-Rose neurons, where each neuron is connected to its nearest neighboring nodes through memristive synapses. Additionally, the network realizes the existence of excitatory and inhibitory coupling by changing the values of memristive synaptic coupling strength. Consequently, we witness several types of traveling chimera states. We find a new traveling chimera state with the coexistence of traveling chimera state and incoherence when the parameters are chosen appropriately. Moreover, we find a new firing pattern named mixed-amplitude bursting state consisting of two bursts with different amplitudes in one firing cycle.

The remainder of this paper is organized as follows. The memristive synaptic Hindmarsh-Rose neuronal network is described, and a statistical measure is introduced in Section 2. The main results regarding the existence of traveling chimera states in the memristive neuronal network with one-way excitatory coupling, bidirectional excitatory coupling, and excitatory-inhibitory coupling, respectively, are clarified in Section 3. An electric circuit is built in Section 4 to regenerate the above results. The conclusions are given in Section 5.

2 Model and method

In this paper, a ring neuronal network with local coupling is constructed, as shown in Figure 1. The N identical Hindmarsh-Rose neurons are selected as the network nodes, and neighboring nodes are connected by memristive synapses. The dynamics of the network are described as the following equations:

$$\begin{aligned}
&\dot{x}_i = a{x_i}^2 - {x_i}^3 - y_i - z_i + \varepsilon_1 M(\varphi_{i-1})(x_{i-1} - x_i) \\
&+\varepsilon_2 M(\varphi_i)(x_{i+1} - x_i), \\
&\dot{y}_i = (a+\alpha){x_i}^2 - y_i, \\
&\dot{z}_i = \mu(bx_i - z_i + c), \\
&\dot{\varphi}_i = x_i - x_{i+1} - \delta\varphi_i,\ i = 1, 2, ..., N,
\end{aligned} \tag{1}$$

where x_i represents the membrane potential of the ith neuron, y_i is the recovery variable, and z_i is the slow current associated with calcium and potassium ions. The parameters a, b, c, μ, and α determine the dynamics of an individual oscillator. The variables φ_i and $M(\varphi_i)$ are the magnetic flux and memductance of the ith memristive synapse, respectively. The cubic order flux-controlled memristor model is expressed as

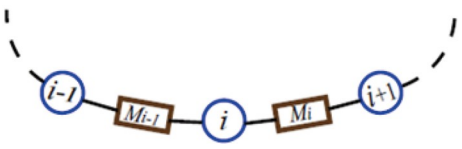

Figure 1 (Color online) Schematic diagram of a memristive neuronal network. The circles and rectangles represent the neurons and memristive synapses, respectively.

$$M(\varphi_i) = \sigma + 3\beta\varphi_i^2, \tag{2}$$

where σ and β describe the memductance, and are related to the environment and their own conditions. The parameter δ contained in the equation of $\dot{\varphi}_i = x_i - x_{i+1} - \delta\varphi_i$ represents the forgetting effect of the memristor; for an ideal memristor, δ = 0. Here, the parameter values σ = 0.12, β = 0.02, δ = 0.5 are fixed at all times. The ring neuronal network satisfies the conditions x_0=x_N and x_{N+1}=x_1 at any moment. Throughout the paper, the parameter values a = 2.8, b = 9, c = 5, μ = 0.001, α = 1.6 are considered to make an isolated neuron in the square-wave bursting state.

The parameters ε_1 and ε_2 are important parts of eq. (1). The ith neuron is connected to the (i+1)th neuron with a coupling strength ε_2 and to the (i−1)th neuron with a coupling strength ε_1. The excitation or inhibition can be achieved by choosing the values of ε_1 and ε_2 [37]. $\varepsilon_1(\varepsilon_2) > 0$ represents an excitatory coupling, while $\varepsilon_1(\varepsilon_2) < 0$ represents an inhibitory coupling. If $\varepsilon_1(\varepsilon_2) = 0$, the neighboring neurons are not coupled. Here, we mainly investigate the existence of chimera states in memristive neuronal networks with one-way local excitatory coupling, excitatory coupling, and excitatory-inhibitory coupling.

The initial conditions for eq. (1) are given as follows: $x_{i0} = 0.05\left(\frac{N}{2} - i\right)$, $y_{i0} = 0.01\left(\frac{N}{2} - i\right)$, $z_{i0} = 0.0151\left(\frac{N}{2} - i\right)$ for $i = 1, 2, ..., \frac{N}{2}$, and $x_{i0} = 0.012\left(i - \frac{N}{2}\right)$, $y_{i0} = 0.02\left(i - \frac{N}{2}\right)$, $z_{i0} = 0.0201\left(i - \frac{N}{2}\right)$ for the remaining neurons. The initial magnetic flux φ_i=0 [36].

Furthermore, the statistical measure of the local order parameter is used to clearly distinguish the incoherent, chimera, and coherent states. The local order parameter reflects the local ordering of neurons, indicating the degree of incoherence and coherence [9,38]. It is defined as follows:

$$L_i = \left| \frac{1}{2p} \sum_{|i-k| \le p} e^{j\Phi_k} \right|, \tag{3}$$

where $j = \sqrt{-1}$, i = 1,2, …, N, and k = 1,2, …, N. The parameter p is the number of nearest neighbors on both sides for the ith node, and Φ_k=arctan(y_k/x_k) is the geometric phase of the kth neuron. If the local order parameter $L_i \approx 0$, the ith neuron belongs to the incoherent group. If $L_i \approx 1$, the ith neuron belongs to a coherent cluster, and a complete coherency is achieved for L_i = 1.

3 Results

3.1 One-way local excitatory coupling

We start with the conditions ε_1=0 and ε_2>0, corresponding to one-way local excitatory coupling. In this case, the ith neuron is only connected to the (i+1)th neuron with the coupling strength ε_2.

We explore the existence of chimera states in one-way local excitatory coupled neuronal networks by varying the memristive coupling strength ε_2. Figure 2 shows the spatiotemporal responses, local order parameters, time series of variables x, and distribution of membrane potentials for ε_2=0.02. 0.18, 1.7 in the neuronal network, respectively. For ε_2 = 0.02, we plot the distribution of membrane potentials at time t = 818 ms as shown in Figure 2(c), where the neurons are divided into two groups with i = 95 as the boundary. The neurons of part I form several coherent clusters, while the distribution of membrane potentials of the neurons of part II is scattered. This indicates that the network is in a chimera state, where coherence and incoherence coexist at time t = 818 ms. However, with an increase in time, the chimera state disappears, and the network finally presents an asynchronous state, as shown in Figure 2(a). This phenomenon is named transient chimera state [39,40]. In Figure 2(d)–(f), the neurons are in an asynchronous state for ε_2 = 0.18. As the memristive coupling strength increases continually to ε_2 = 1.7, the neurons are divided into three coherent and two incoherent groups, and the synchronous state of neurons will change over time, implying that the network is in a traveling chimera state. We also compute the local order parameter L_i of neurons for a long time interval (Figure 2(b), (e) and (h)), which accords well with the above findings. Moreover, changing the memristive coupling strength ε_2 can change not only the synchronous state of the network but also the firing pattern of neurons. As shown in Figure 2(c), (f) and (i), square wave bursting, plateau bursting, and irregular plateau bursting states successively appear with the change of synaptic coupling strength.

Then, we convert the memristive synaptic coupling strengths ε_1 and ε_2 such that ε_2 = 0, and change the value of ε_1. Figure 3 shows the spatiotemporal plots and distribution of membrane potentials of neurons for ε_1=2.15, 2.75. In Figure 3(a), the spatiotemporal plot exhibits two combined states with i = 100 as the boundary. Neurons with indices from i = 1 to i = 100 are in a traveling chimera state, while the others are in an incoherent state. We name the special phenomenon observed in the memristive neuronal network as the semi-traveling chimera state. On continually increasing the value of ε_1, we observe a global traveling chimera state in the network (Figure 3(b)). Interestingly, the directions of traveling chimera states are opposite to those in Figure 2. In Figure 2, ε_1 = 0 and ε_2 > 0, while in Figure 3, ε_1 > 0 and ε_2 = 0. Thus, changes in the traveling direction of the traveling chimera state may relate to the transmission direction of the excitatory coupling in the network.

3.2 Excitatory coupling

In this part, we investigate the dynamics of chimera state in

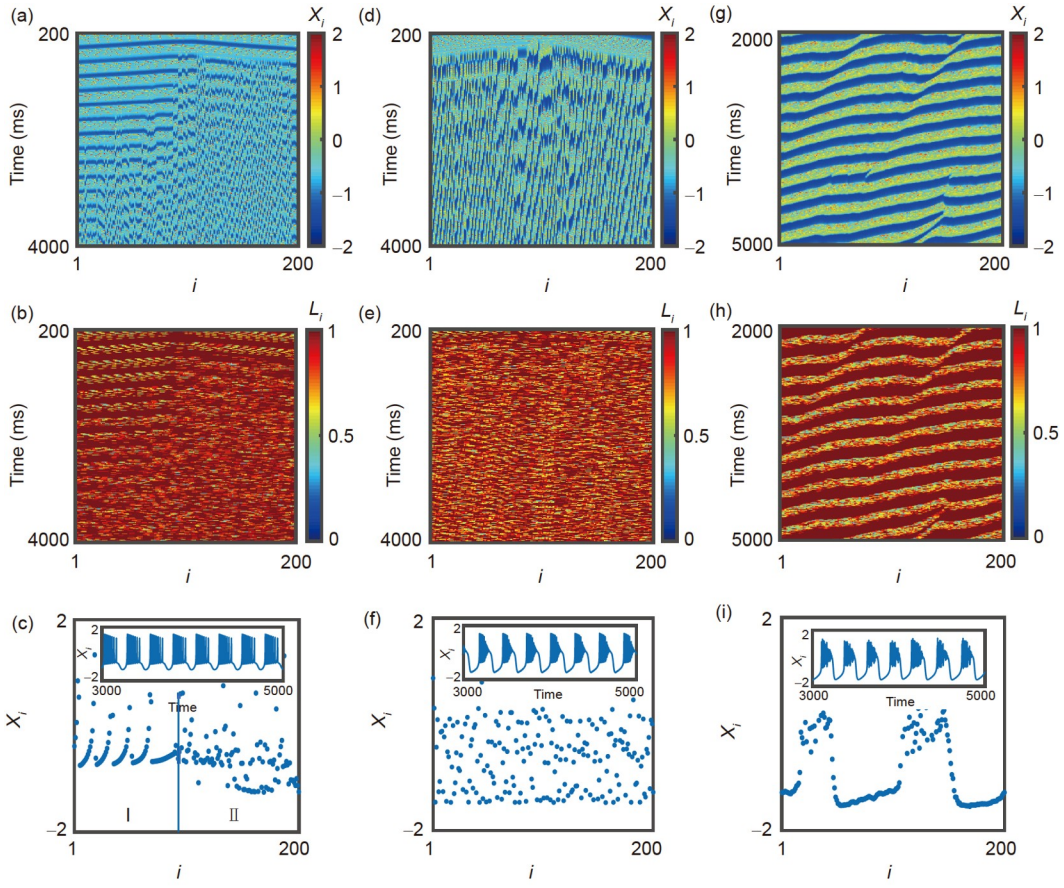

Figure 2 Snapshots of one-way locally excitatory coupled memristive neuronal network with $\varepsilon_1 = 0$ and $\varepsilon_2 > 0$. (a)–(c) Transient chimera state, $\varepsilon_2 = 0.02$; (d)–(f) incoherent state, $\varepsilon_2 = 0.18$; (g)–(i) traveling chimera state, $\varepsilon_2 = 1.7$. (a), (d), (g) Reflect upon the spatiotemporal plots for neuron indices $i = 1, 2, \ldots, N$; (b), (e), (h) the local order parameters; (c), (f), (i) the time series and the distribution of membrane potentials of $N = 200$ neurons.

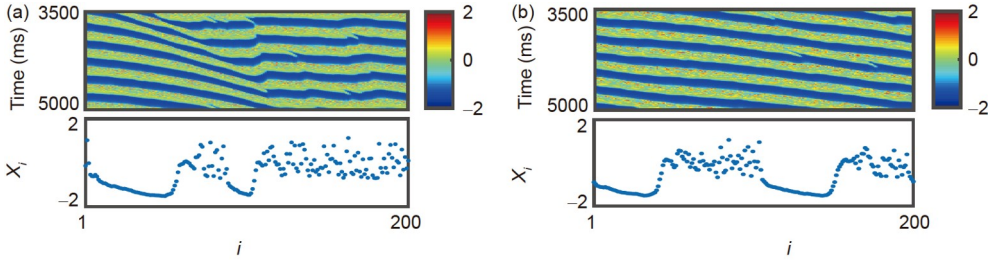

Figure 3 Spatiotemporal plots and distribution of membrane potentials of one-way excitatory coupled neurons for $\varepsilon_1 > 0$ and $\varepsilon_2 = 0$. (a) Semi-traveling chimera state, $\varepsilon_1 = 2.15$; (b) traveling chimera state, $\varepsilon_1 = 2.75$.

excitatory coupled neuronal network with $\varepsilon_1 > 0$ and $\varepsilon_2 > 0$. The ith neuron is connected to the $(i-1)$th neuron with a memristive synaptic coupling strength ε_1 and to the $(i+1)$th neuron with the coupling strength ε_2, so that a bidirectional excitatory connection can be set up.

On changing the values of ε_1 and ε_2, we observe several types of traveling chimera states, and the difference among them is the number of coherent and incoherent groups contained in traveling chimera states, as shown in Figure 4. The upper part of each picture shows the spatiotemporal response of neurons, and the lower part shows the distribution of membrane potentials at $t = 5000$ ms. The neurons in the network are divided into several coherent groups and incoherent groups, a phenomenon named multi-head traveling chimera state [36], with the chimera's heads referring to the number of incoherent groups. By fixing $\varepsilon_1 = 0.8$ and varying ε_2, it is found that for a small value of $\varepsilon_2 = 3.6$, the network is in a traveling chimera state with two incoherent groups, which we term as the two-head traveling chimera state (Figure 4(a)). For a large value of $\varepsilon_2 = 3.9$, the three-head traveling chimera state appears in the neuronal network (Figure 4(b)). Similarly, Figure 4(c) and (d) show other

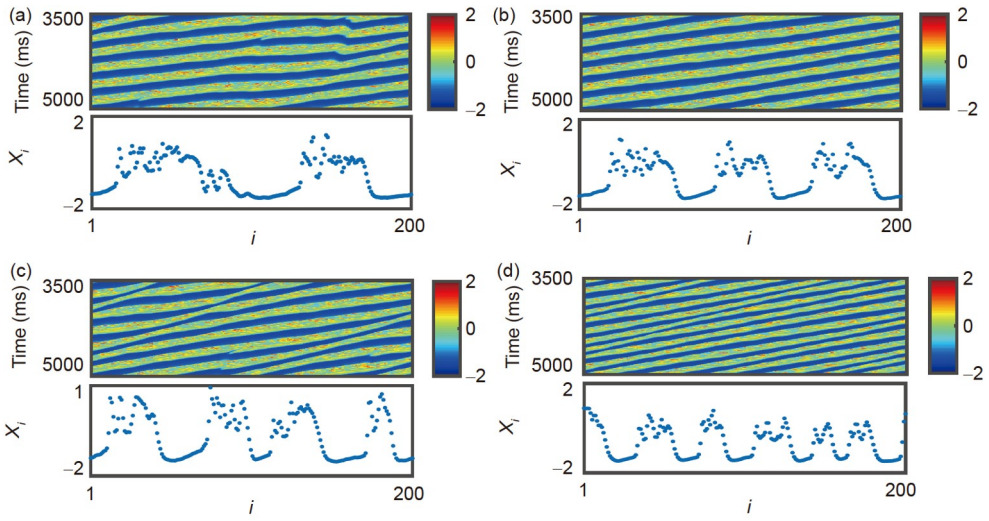

Figure 4 Snapshots of spatiotemporal responses and distribution of membrane potentials of neurons for different values of ε_1 and ε_2 in the excitatory coupled network. (a) Two-head traveling chimera state, $\varepsilon_2 = 3.6$; (b) three-head traveling chimera state, $\varepsilon_2 = 3.9$; (c) four-head traveling chimera state, $\varepsilon_2 = 4.0$; (d) six-head traveling chimera state, $\varepsilon_2 = 6.0$. (a), (b) $\varepsilon_1 = 0.8$; (c), (d) $\varepsilon_1 = 1.0$.

patterns of traveling chimera states with additional incoherent clusters. This unique state of the neuronal network may relate to a special information transfer mechanism.

Multi-head chimera states are composed of several incoherent and coherent clusters. To explore the influence and law of memristive synaptic coupling strengths ε_1 and ε_2 on the number of coherent clusters of traveling chimera states, we plot the graphs of the relationship between ε_1, ε_2, and the number of coherent groups, as shown in Figure 5. The number 0 on the vertical axis indicates that the network is in an incoherent state. Memristive synaptic coupling strength ε_2 is set in the range (2, 10). Figure 5(a)–(d) correspond to $\varepsilon_1 = 0.2$, 0.5, 0.8, and 1.0, respectively. Multi-head chimera states appear in Figure 5, and the numbers of coherent groups of traveling chimera states are concentrated to 4, 5, and 6. However, the difference is that for a larger ε_1, a larger ε_2 is also required for the occurrence of multi-head traveling chimera state, as seen by comparing Figure 5(a) and (d).

3.3 Excitatory-inhibitory coupling

Here, we study the dynamics in the memristive synaptic

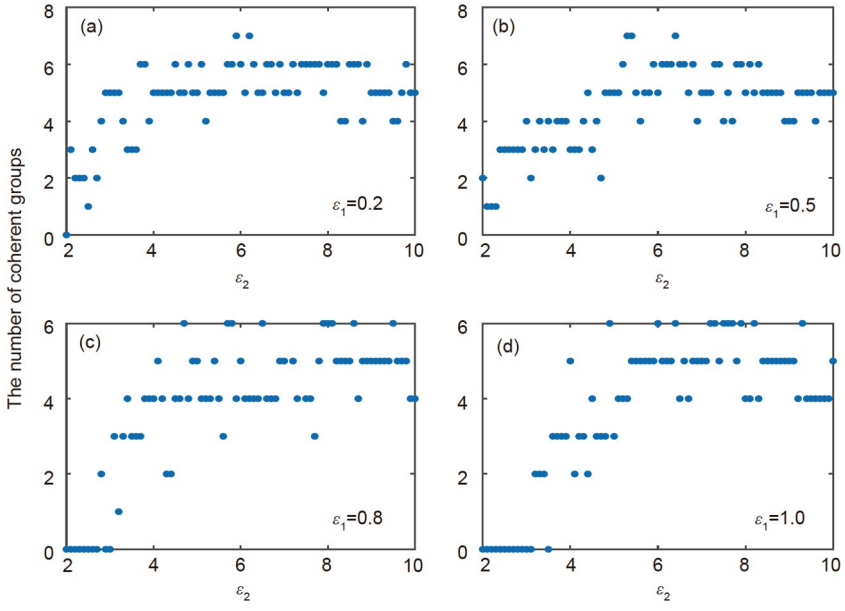

Figure 5 The number of coherent groups of the multi-head traveling chimera states for different values of memristive synaptic coupling strengths ε_1 and ε_2. (a) $\varepsilon_1 = 0.2$; (b) $\varepsilon_1 = 0.5$; (c) $\varepsilon_1 = 0.8$; (d) $\varepsilon_1 = 1.0$. Here $N = 200$, $\varepsilon_2 \in (2, 10)$.

coupled neuronal network with excitatory-inhibitory coupling. To connect the ith neuron and the $(i-1)$th neuron via inhibitory synapses, and the ith neuron and the $(i+1)$th neuron via excitatory synapses, we set $\varepsilon_1<0$ and $\varepsilon_2>0$, respectively.

Several types of firing patterns are discovered when the network is in incoherent states. Figure 6 shows the snapshots of the distribution and time series of membrane potentials of all neurons. First, we fix the value of ε_2 and obtain the results. For a weak inhibitory coupling strength of $\varepsilon_1=-0.01$, the neurons exhibit a square wave bursting state (Figure 6(a)). For a stronger inhibitory coupling strength of $\varepsilon_1=-0.4$, the time sequences of the spiking state of neurons are shown in Figure 6(b). In this paper, we set the initial state of the firing pattern as a bursting state; however, a spiking state appears in the network in an incoherent state. This is counter-intuitive and may relate to the properties of memristive synapses. Then, on continuously changing the synaptic coupling strengths to $\varepsilon_1=-0.4$ and $\varepsilon_2=0.38$, we observe an irregular bursting state (Figure 6(c)). The time sequences of membrane potentials are composed of two types of bursts, one with a larger amplitude and the other with a smaller amplitude. We name this time series of membrane potentials a mixed-amplitude bursting state.

Moreover, we discover traveling chimera states in the memristive neuronal network with excitatory-inhibitory coupling. The membrane potentials from t = 3500 ms to t = 5000 ms for all Hindmarsh-Rose neurons are recorded and analyzed. In Figure 7, we fix $\varepsilon_1=-1$ and vary the value of ε_2. For $\varepsilon_1=2.8$, we observe a four-head traveling chimera state, and the firing pattern of each neuron is in an irregular plateau bursting state shown in Figure 7(a). As the value of ε_2 increases to 50, the system exhibits strong excitatory coupling and weak inhibitory coupling. The snapshots of a memristive neuronal network show spatiotemporal responses of all neurons with regular edges. In this type of traveling chimera states, only a few neurons are in the incoherent group, as shown in Figure 7(b). Moreover, we calculate the local order parameter L_i, and almost the entire plane shows L_i = 1; thus, this state can also be called an imperfect coherent state. Meanwhile, the time sequences of the membrane potentials of neurons in the network also change, with the spikes de-

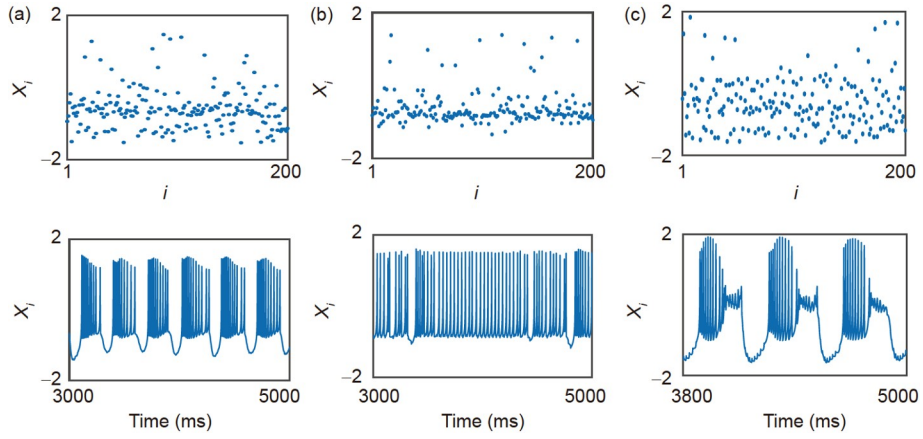

Figure 6 Snapshots of the distribution and time series of membrane potentials in networks with excitatory-inhibitory coupling. (a)–(c) All incoherent states. (a) Square wave bursting state, $\varepsilon_1 = -0.1$, $\varepsilon_2 = 0.1$; (b) spiking firing state, $\varepsilon_1 = -0.4$, $\varepsilon_2 = 0.1$; (c) mixed-amplitude bursting state, $\varepsilon_1 = -0.4$, $\varepsilon_2 = 0.38$.

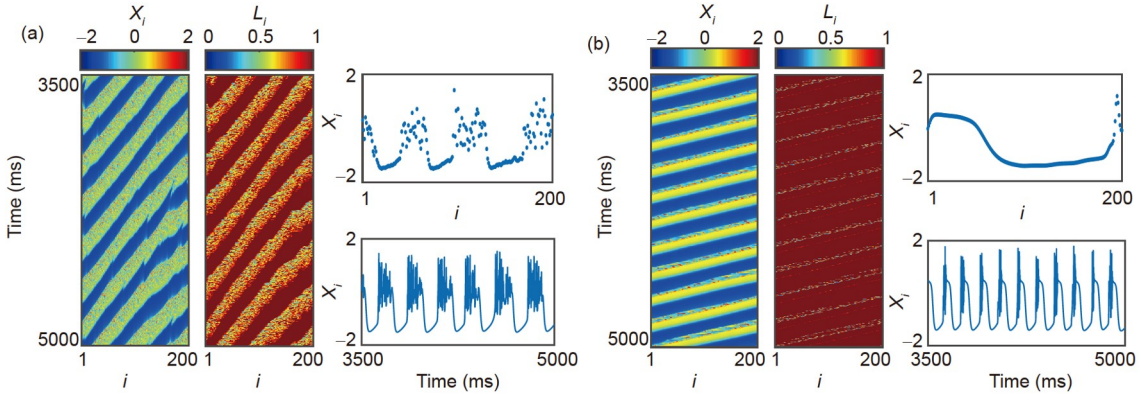

Figure 7 Snapshots of two types of traveling chimera states. (a) Traveling chimera state, $\varepsilon_2 = 2.8$; (b) imperfect coherent state, $\varepsilon_2 = 50$. Here $\varepsilon_1 = -1$, $N = 200$.

creasing in a burst. The results show that the larger excitatory coupling strength can promote the synchronization of neurons and the interaction of ε_1 and ε_2 can induce various firing patterns.

To clearly show the spatiotemporal dynamics of the memristive neuronal network with local coupling, we plot the two-parameter (ε_1, ε_2) phase diagram, as shown in Figure 8. For the range of $\varepsilon_1 \in (-1, 1)$ and $\varepsilon_2 \in (-1, 3)$, the entire plane is divided into three regions: incoherent, chimera, and transient chimera states. In a two-way inhibition ($\varepsilon_1<0$ and $\varepsilon_2<0$), there is no stably persistent chimera state. The transient chimera state appears in the range of $\varepsilon_1 \approx 0$ and $\varepsilon_2 \approx 0$, indicating that weak interactions between neurons cannot maintain stable chimera states or make the network with a large incoherent domain. Eventually, the neurons collapse into an incoherent state. Moreover, it is obvious that in the case of excitatory–inhibitory coupling, as the inhibition becomes stronger, the system needs a larger excitatory coupling strength to achieve the chimera state. Thus, it can be concluded that the inhibitory coupling can inhibit the network switching to a synchronized state.

4 Electric circuit design and simulation

In this section, an analog circuit of a locally coupled memristive neuronal network composed of 20 Hindmarsh-Rose neurons is constructed on Multisim.

To facilitate the design and analysis, all variables of eq. (1) are represented by electric potentials in the circuit. The memristive synaptic coupling strengths ε_1 and ε_2 are represented by *Vesp*1(*esp*1) and *Vesp*2(*esp*2), respectively, as shown in Figure 9. The structures of a single Hindmarsh-Rose neuron, a memristive synapse, and the input current of a neuron are encapsulated as the Neu*i*, Syn*I*, and TotalI blocks, respectively (Figure 10). The circuit diagram of a single Hindmarsh-Rose neuron is shown in Figure 10(a), where the voltages of the capacitors CX, CY, and CZ represent the state variables x, y, and z of the Hindmarsh-Rose neuron model, respectively. The variable i of the block represents the total input current of a neuron, and the output x represents the membrane potential. From the Hindmarsh-Rose model and the analog circuit based on the operational amplifiers, the following equations are obtained:

$$\begin{aligned}
\dot{x} &= R_{x6}\left(\frac{x^2}{R_{x1}} - \frac{x^3}{R_{x2}} - \frac{y}{R_{x3}} - \frac{z}{R_{x4}} + \frac{I}{R_{x5}}\right),\\
\dot{y} &= R_{y3}\left(\frac{x^2}{R_{y1}} - \frac{y}{R_{y2}}\right),\\
\dot{z} &= R_{z4}\left(\frac{x}{R_{z1}} - \frac{z}{R_{z3}} + \frac{V_z}{R_{z2}}\right).
\end{aligned} \tag{4}$$

All capacitance and resistance values in the integration circuit of all operational amplifiers are fixed: $C = 50nF$ and $R = 20\ \mathrm{k\Omega}$. Then, the relationship between input and output of the integration circuit is as follows:

$$u_{\mathrm{out}} = -\frac{1}{RC}\int u_{\mathrm{in}}\mathrm{d}t. \tag{5}$$

The structure of the memristive synapse is shown in Figure 10(b). The inputs x_i and x_{i+1} of the block are the membrane potentials of the ith and $(i+1)$th neurons, respectively, and the output $I_{\mathrm{Syn}}(i)=M(\varphi_i)(x_i-x_{i+1})$. The magnetic flux and the memductance can be expressed as

$$\begin{aligned}
\dot{\varphi}_i &= R_{SA3}\left(\frac{x_i - x_{i+1}}{R_{SA1}} + \frac{\varphi_i}{R_{SA2}}\right),\\
M(\varphi_i) &= R_{SA6}\left(\frac{\varphi_i^2}{R_{SA4}} + \frac{V_1}{R_{SA5}}\right).
\end{aligned} \tag{6}$$

The circuit of a single neuron receiving current is shown in Figure 10(c). The inputs I_{Si} and I_{Si-1} represent the current from the ith synapse and the $(i-1)$th synapse to the ith neuron. The variables *esp*1 and *esp*2 represent the memristive synaptic coupling strengths ε_1 and ε_2, respectively.

By changing the values of memristive coupling strengths *Veps*1 and *Veps*2 in Figure 9, the excitatory and inhibitory connections of the network can be realized. We set the simulation step size as 0.001 s, run the circuit, and monitor the membrane potentials of neurons for a long time interval; the data of membrane potentials of all neurons are recorded by using the function of transient analysis on Multisim. We import the data from Multisim into MATLAB and plot the graphs of spatiotemporal responses and the distribution of membrane potentials of neurons (Figure 11). First, for *Veps*1 = 0 and *Veps*2 = 0, each neuron is in an isolated state and should present a square wave bursting state, and the simulation results are as expected, as shown in Figure 11(a). Then, for *Veps*1 = 0 & *Veps*2 = 0.5 and *Veps*1 = 0.6 & *Veps*2 = 0.2, the results (Figure 11(b) and (c)) corresponds well to the cases of one-way excitatory coupling and bidirectional excitatory coupling in Figures 2 and 4, respectively. The neurons are organized into traveling chimera states and exhibit plateau bursting states. Finally, for *Veps*1 = 1.5 and *Veps*2 =

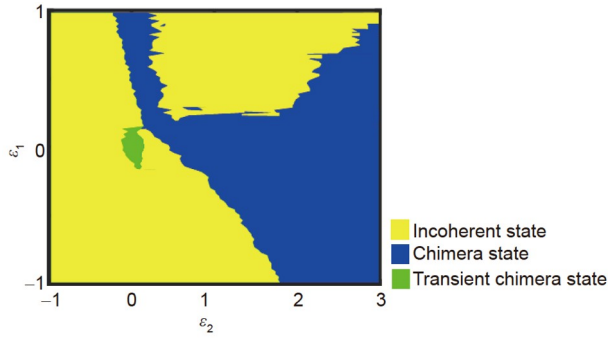

Figure 8 Two-parameter (ε_1, ε_2) phase diagram for a locally coupled memristive network of $N = 200$ identical Hindmarsh-Rose oscillators. The yellow, blue, and green regions represent the incoherent, chimera, and transient chimera states, respectively.

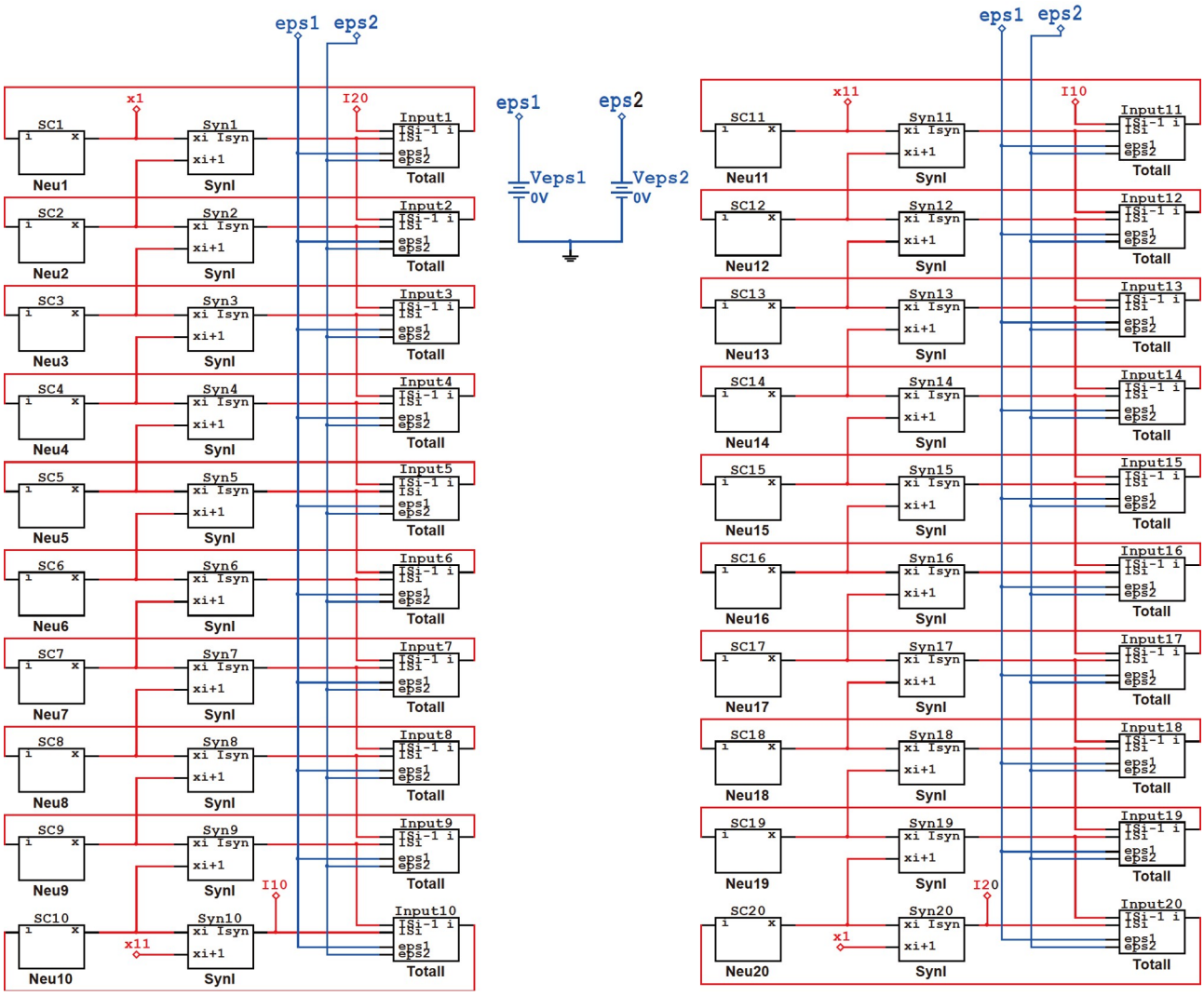

Figure 9 Electric circuit of a memristive neuronal network of 20 coupled Hindmarsh-Rose neurons.

−0.25, the coupling mode of the memristive network is the excitatory-inhibitory connection. The network presents a traveling chimera state, and the time series of the membrane potential of a single neuron is recorded in Figure 11(d), in accordance with the snapshots in Figure 7. The results of circuit simulation further confirm that the magnitude of synaptic coupling strength, inhibition, and excitation can affect the traveling direction of a traveling chimera state. Our work also verifies that traveling chimera states can arise in real circuits and may provide a new idea for further study of chimera states.

5 Conclusion

In this paper, a model of memristive neuronal network with locally excitatory and inhibitory coupling is proposed. The ith neuron connects the $(i-1)$th and $(i+1)$th neuron by two variables of memristive synaptic coupling strengths, and we investigate the existence of traveling chimera states in the network. The results show that the interaction of synaptic coupling strengths ε_1 and ε_2 can induce not only various modes of traveling chimera states but also firing patterns of neurons in the excitatory and inhibitory locally coupled neuronal networks. For weak interactions among the neurons, the network has a large incoherent domain, while the strong interactions make the system have a large basin of attraction for chimera states. Interestingly, in the one-way locally excitatory coupling, we observe a transient chimera state, eventually collapsing into an incoherent state. A new type of chimera pattern consisting of a traveling chimera state and an incoherent state is defined as the semi-traveling chimera state. In a network with bidirectional excitatory local coupling, the neurons show multi-head traveling chimera states with different numbers of incoherent groups by suitably changing the memristive coupling strength. Further-

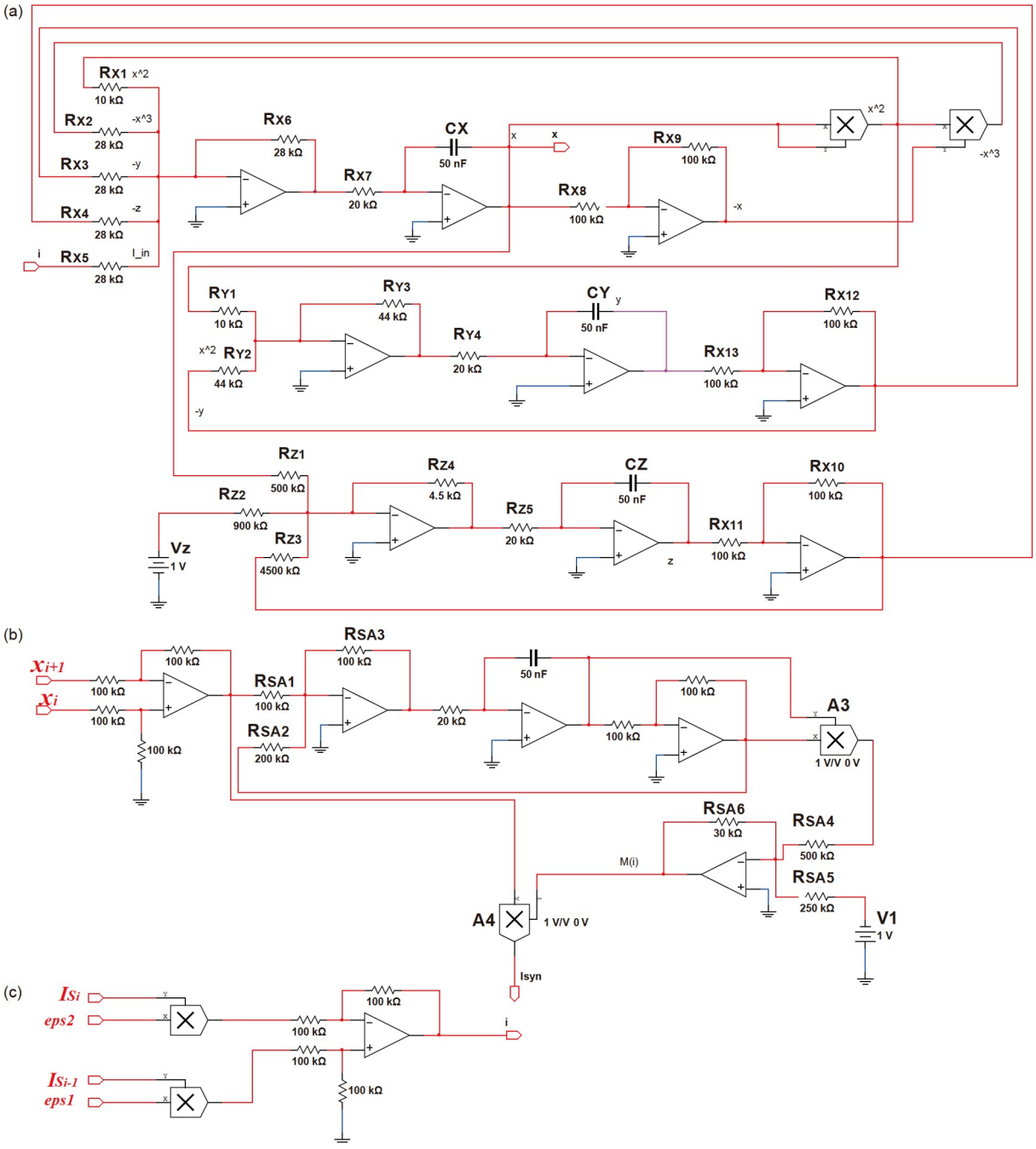

Figure 10 (Color online) Three blocks contained in an electric circuit. (a) Neu*i*: structure of a single Hindmarsh-Rose neuron; (b) Syn*I*: structure of a memristive synapse; (c) TotalI: input current of a neuron.

more, as the memristive synaptic coupling strength varies, the firing pattern of neurons changes from square-wave bursting to plateau bursting. In the excitatory-inhibitory coupling, for strong excitatory connection and weak inhibitory connection between the neighboring nodes, we observe a traveling chimera state with regular edges and the neurons of the network almost in a coherent state, which is imperfect. Moreover, we observe a mixed-amplitude bursting pattern whose burst consists of two different amplitudes when the network is in an incoherent state. Meanwhile, incoherent and chimera states are distinguished by using the statistical measure of the local order parameter. Conclusively, our work confirms that in locally coupled memristive neuronal networks, various dynamical behaviors can be realized by regulating coupling modes appropriately. We also confirm the above results for a smaller ($N = 100$) size of the Hindmarsh–Rose neuronal network, ensuring that our results are applicable to other sizes of networks as well. Finally, we design a neural circuit to regenerate the above phenomena, and the results accord well with our findings,

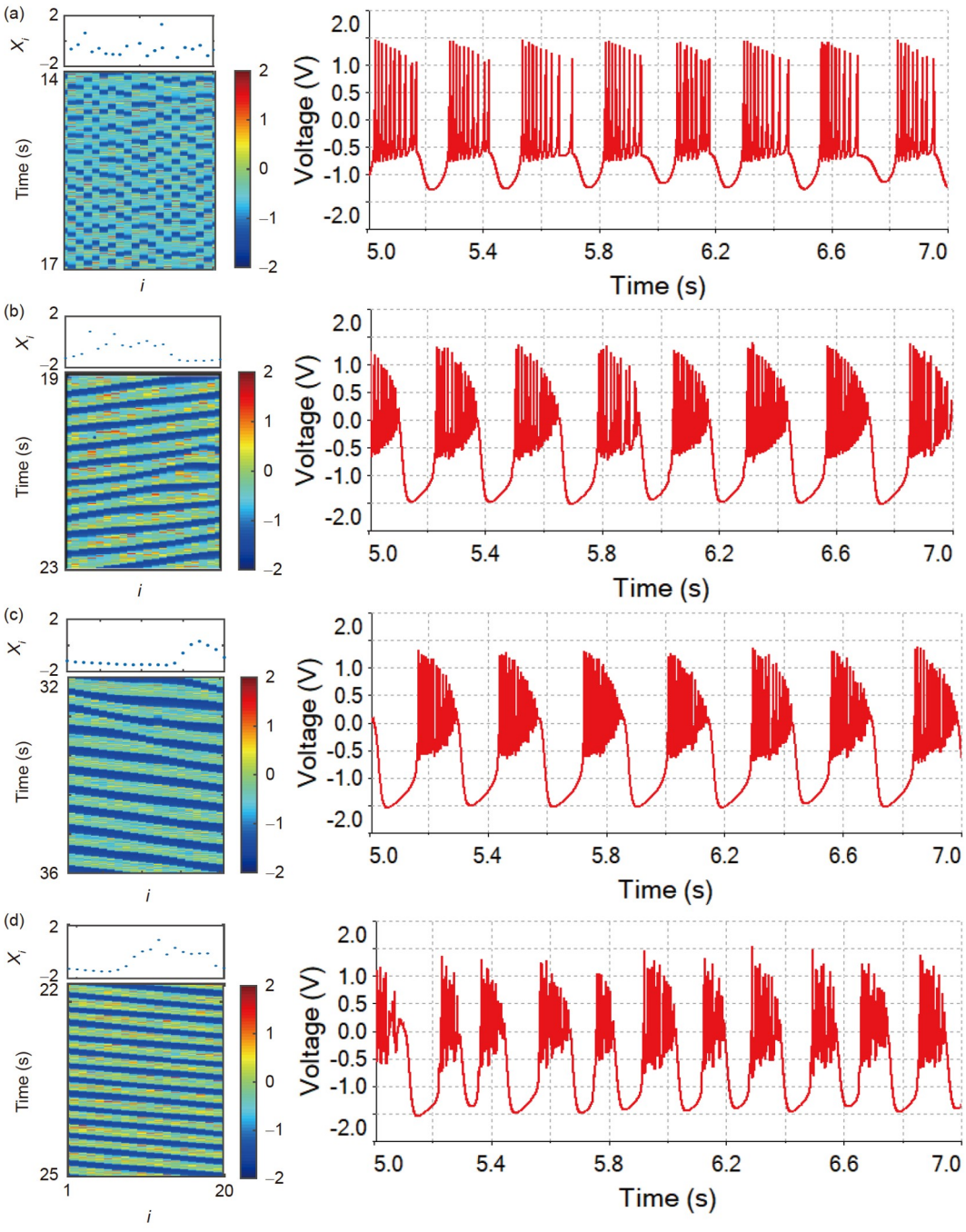

Figure 11 Snapshots of spatiotemporal responses, distribution, and time series of the membrane potentials of neurons. (a) Incoherent state; (b)–(d) traveling chimera states. (a) Each neuron is in an isolated state, *Veps*1 = 0 and *Veps*2 = 0; (b) one-way local excitatory coupling, *Veps*1 = 0 and *Veps*2 = 0.5; (c) bidirectional excitatory coupling, *Veps*1 = 0.6 and *Veps*2 = 0.2; (d) excitatory-inhibitory coupling, *Veps*1 = 1.5 and *Veps*2 = −0.25. Here $N = 20$.

indicating that chimera states in memristive neuronal networks could be realized by circuits. Our study could be used to control the dynamical behaviors of memristive neuronal networks and may provide clues for constructing artificial neural systems.

This work was supported by the National Natural Science Foundation of China (Grant No. 11972115) and the Fundamental Research Funds for the Central Universities.

1 Kuramoto Y, Battogtokh D. Coexistence of coherence and incoherence in nonlocally coupled phase oscillators. Nonlinear Phenom Complex Syst, 2002, 5: 380385
2 Abrams D M, Strogatz S H. Chimera states in a ring of nonlocally coupled oscillators. Int J Bifurcation Chaos, 2006, 16: 21–37
3 Kawamura Y. Chimera Ising walls in forced nonlocally coupled oscillators. Phys Rev E, 2007, 75: 056204
4 Premalatha K, Chandrasekar V K, Senthilvelan M, et al. Impact of symmetry breaking in networks of globally coupled oscillators. Phys Rev E, 2015, 91: 052915
5 Singha J, Gupte N. Chimera states in globally coupled sine circle map

lattices: Spatiotemporal intermittency and hyperchaos. Phys Lett A, 2020, 384: 126225
6 Bera B K, Ghosh D. Chimera states in purely local delay-coupled oscillators. Phys Rev E, 2016, 93: 052223
7 Gambuzza L V, Minati L, Frasca M. Experimental observations of chimera states in locally and non-locally coupled Stuart-Landau oscillator circuits. Chaos Soliton Fract, 2020, 138: 109907
8 Dudkowski D, Czołczyński K, Kapitaniak T. Multi-headed loop chimera states in coupled oscillators. Chaos, 2021, 31: 013135
9 Bera B K, Ghosh D, Banerjee T. Imperfect traveling chimera states induced by local synaptic gradient coupling. Phys Rev E, 2016, 94: 012215
10 Simo G R, Louodop P, Ghosh D, et al. Traveling chimera patterns in a two-dimensional neuronal network. Phys Lett A, 2021, 409: 127519
11 Sethia G C, Sen A, Johnston G L. Amplitude-mediated chimera states. Phys Rev E, 2013, 88: 042917
12 Zakharova A, Kapeller M, Schöll E. Chimera death: Symmetry breaking in dynamical networks. Phys Rev Lett, 2014, 112: 154101
13 Shepelev I A, Bukh A V, Strelkova G I, et al. Chimera states in ensembles of bistable elements with regular and chaotic dynamics. Nonlinear Dyn, 2017, 90: 2317–2330
14 Kasatkin D V, Yanchuk S, Schöll E, et al. Self-organized emergence of multilayer structure and chimera states in dynamical networks with adaptive couplings. Phys Rev E, 2017, 96: 062211
15 Calim A, Torres J J, Ozer M, et al. Chimera states in hybrid coupled neuron populations. Neural Netw, 2020, 126: 108–117
16 Tognoli E, Kelso J A S. The metastable brain. Neuron, 2014, 81: 35–48
17 Hizanidis J, Kouvaris N E, Zamora-López G, et al. Chimera-like states in modular neural networks. Sci Rep, 2016, 6: 19845
18 Santos M S, Szezech J D, Borges F S, et al. Chimera-like states in a neuronal network model of the cat brain. Chaos Soliton Fract, 2017, 101: 86–91
19 Provata A, Venetis I E. Chimera states in Leaky Integrate-and-Fire dynamics with power law coupling. Eur Phys J B, 2020, 93: 160
20 Fan D G, Wang Q Y. Synchronization and bursting transition of the coupled Hindmarsh-Rose systems with asymmetrical time-delays. Sci China Technol Sci, 2017, 60: 1019–1031
21 Bera B K, Ghosh D, Lakshmanan M. Chimera states in bursting neurons. Phys Rev E, 2016, 93: 012205
22 Wang Z, Xu Y, Li Y, et al. Chimera states in coupled Hindmarsh-Rose neurons with α-stable noise. Chaos Soliton Fract, 2021, 148: 110976
23 Simo G R, Njougouo T, Aristides R P, et al. Chimera states in a neuronal network under the action of an electric field. Phys Rev E, 2021, 103: 062304
24 Ruzzene G, Omelchenko I, Sawicki J, et al. Remote pacemaker control of chimera states in multilayer networks of neurons. Phys Rev E, 2020, 102: 052216
25 Tang J, Zhang J, Ma J, et al. Noise and delay sustained chimera state in small world neuronal network. Sci China Tech Sci, 2019, 62: 1134–1140
26 Majhi S, Perc M, Ghosh D. Chimera states in a multilayer network of coupled and uncoupled neurons. Chaos, 2017, 27: 073109
27 Eichler S A, Meier J C. E-I balance and human diseases – From molecules to networking. Front Mol Neurosci, 2008, 1: 2
28 Belykh I, Reimbayev R, Zhao K. Synergistic effect of repulsive inhibition in synchronization of excitatory networks. Phys Rev E, 2015, 91: 062919
29 Wang X, Hou Z, Yu W, et al. Online scale adaptive visual tracking based on multilayer convolutional features. IEEE Trans Cybern, 2019, 49: 146–158
30 Ma J, Tang J. A review for dynamics in neuron and neuronal network. Nonlinear Dynam, 2017, 89: 1569–1578
31 Xu Y, Jia Y, Ma J, et al. Synchronization between neurons coupled by memristor. Chaos Soliton Fract, 2017, 104: 435–442
32 Ma J, Mi L, Zhou P, et al. Phase synchronization between two neurons induced by coupling of electromagnetic field. Appl Math Computation, 2017, 307: 321–328
33 Korneev I A, Semenov V V, Slepnev A V, et al. The impact of memristive coupling initial states on travelling waves in an ensemble of the FitzHugh–Nagumo oscillators. Chaos Soliton Fract, 2021, 147: 110923
34 Bao H, Zhang Y, Liu W, et al. Memristor synapse-coupled memristive neuron network: Synchronization transition and occurrence of chimera. Nonlinear Dyn, 2020, 100: 937–950
35 Liu Y, Sun Z, Yang X, et al. Dynamical robustness and firing modes in multilayer memristive neural networks of nonidentical neurons. Appl Math Comput, 2021, 409: 126384
36 Xu F, Zhang J, Jin M, et al. Chimera states and synchronization behavior in multilayer memristive neural networks. Nonlinear Dynam, 2018, 94: 775–783
37 Sakaguchi H. Instability of synchronized motion in nonlocally coupled neural oscillators. Phys Rev E, 2006, 73: 031907
38 Omelchenko I, Omel'chenko O E, Hövel P, et al. When nonlocal coupling between oscillators becomes stronger: Patched synchrony or multichimera states. Phys Rev Lett, 2013, 110: 224101
39 Wolfrum M, Omel'chenko O E. Chimera states are chaotic transients. Phys Rev E, 2011, 84: 015201
40 Lilienkamp T, Parlitz U. Susceptibility of transient chimera states. Phys Rev E, 2020, 102: 032219